

## RESEARCH ARTICLE



## OPEN ACCESS

Received: 30-06-2022

Accepted: 23-09-2022

Published: 03-11-2022

**Citation:** Hoang L, Vu AT (2022) Preparation of Novel Triangular Prism  $\epsilon$ -Zn(OH)<sub>2</sub> by the Facile Precipitation Route for the Photocatalysis Under Visible Light. Indian Journal of Science and Technology 15(41): 2143-2150. <https://doi.org/10.17485/IJST/v15i41.1368>

\* Corresponding author.

tuan.vuanh@hust.edu.vn

**Funding:** Vietnam National Foundation for Science and Technology Development (NAFOSTED) under grant number 104.05-2018.333

**Competing Interests:** None

**Copyright:** © 2022 Hoang & Vu. This is an open access article distributed under the terms of the [Creative Commons Attribution License](#), which permits unrestricted use, distribution, and reproduction in any medium, provided the original author and source are credited.

Published By Indian Society for Education and Environment ([iSee](#))

**ISSN**

Print: 0974-6846

Electronic: 0974-5645

# Preparation of Novel Triangular Prism $\epsilon$ -Zn(OH)<sub>2</sub> by the Facile Precipitation Route for the Photocatalysis Under Visible Light

Lam Hoang<sup>1</sup>, Anh-Tuan Vu<sup>1\*</sup>

<sup>1</sup> School of Chemical Engineering, Hanoi University of Science and Technology, Hanoi, Viet Nam

## Abstract

**Objective:** This study aims to decompose antibiotic of tetracycline hydrochloride (TCH) in aqueous medium by photocatalysis under the visible light irradiation. **Method:** Photocatalyst  $\epsilon$ -Zn(OH)<sub>2</sub> was synthesized by facile precipitation method from an aqueous containing zinc nitrate, using trisodium citrate dihydrate. The characterization of as-prepared material was confirmed by XRD, SEM, FT-IR, and UV-Vis-DR. The catalytic performance of catalyst was evaluated by batch reaction. **Finding:**  $\epsilon$ -Zn(OH)<sub>2</sub> has an orthorhombic structure with a length prism of 5-7  $\mu$ m and triangle angles of 56.92, 69.46, and 66.71°.  $\epsilon$ -Zn(OH)<sub>2</sub> has been shown to efficiently degrade tetracycline hydrochloride. The degradation efficiency (DE) and reaction rate at the TCH concentration of 5 mg/L were the highest, exhibiting 89.51% and 0.120 min<sup>-1</sup>, respectively. The alkaline medium was an appropriate condition for degradation of TCH on catalyst. **Application/Improvement:**  $\epsilon$ -Zn(OH)<sub>2</sub> was synthesized by the facile precipitation method, it has relatively strong photocatalytic ability for applying in treatment of medical wastewater. **Novelty:** Novel triangular prism  $\epsilon$ -Zn(OH)<sub>2</sub> was prepared for photocatalysis. The relationship between structure and catalytic efficiency was investigated in detail. In addition, the photocatalytic mechanism of TCH on  $\epsilon$ -Zn(OH)<sub>2</sub> has been proposed.

**Keywords:** Photocatalyst; Zn(OH)<sub>2</sub>; Tetracycline hydrochloride; Degradation; Kinetic

## 1 Introduction

The antibiotic tetracyclines were discovered in 1948, and soon it has been commercialized for clinical applications. Tetracyclines have been among the most widely used broad-spectrum antibiotics for bacterial infections in humans and animals<sup>(1)</sup>. However, the indiscriminate use as well as the excessive consumption of tetracyclines, leading many threats to the whole eco-system and humans<sup>(2)</sup>. As a result, it imperatively needs techniques to remove pharmaceutical antibiotics-containing wastewater. There have been various methods developed by researchers to eliminate antibiotics such as

adsorption<sup>(3)</sup>, reverse osmosis<sup>(4)</sup>, advanced oxidation process<sup>(5)</sup>, and photocatalytic techniques<sup>(6-8)</sup>. Among these methods, photocatalyst has been widely used in recent years due to its the eco-friendly operation, inexpensive, and non-toxicity.

Recently, various metal-oxide semiconductors have been used to photodegrade antibiotics. Zinc-based nanomaterial has emerged as one of the most suitable materials for this process. Among these, ZnO has been studied and applied in many fields. However, other compounds such as zinc hydroxide  $\text{Zn(OH)}_2$ , and zinc hydroxyfluorides  $\text{Zn(OH)F}$  were poorly investigated.  $\text{Zn(OH)}_2$  is an amphoteric compound, which has different lattice structures: tetrahedral, hexagonal, and orthorhombic<sup>(9)</sup>. Besides, it is an important precursor for the growth of ZnO.  $\text{Zn(OH)}_2$  has been an absorbent in medical-surgical dressings. Hence, it is rarely used as a photocatalytic.

ZnO base materials are often used as photocatalysts to degrade toxic organic matter in water, while little research has been done on triangular prism  $\text{Zn(OH)}_2$  for the catalytic process. In this study, a simple precipitation method was used to synthesize triangular prism  $\text{Zn(OH)}_2$ . The batch reaction was studied to model the degradation reaction of tetracycline hydrochloride in wastewater. Optimal conditions for catalysis were demonstrated through experiments involving pH and tetracycline hydrochloride concentration. The first-order kinetic plot was used to calculate the rate constant of reaction

## 2 Methodology

### 2.1 Materials

Zinc nitrate hexahydrate ( $\text{Zn(NO}_3)_2 \cdot 6\text{H}_2\text{O}$ , 99%), trisodium citrate dihydrate ( $\text{C}_6\text{H}_5\text{Na}_3\text{O}_7 \cdot 2\text{H}_2\text{O}$ , 99%), and sodium hydroxide (NaOH, 96%) were purchased Xiong scientific Co., Ltd, China. Tetracycline hydrochloride ( $\text{C}_{22}\text{H}_{24}\text{N}_2\text{O}_8 \cdot \text{HCl}$ , 99%) was purchased HeFei BoMei Biotechnology Co., Ltd, China. All the chemicals were used without any purification and distilled water was used in all experiments.

### 2.2 Synthesis of $\text{Zn(OH)}_2$

The triangular prism  $\text{Zn(OH)}_2$  synthesis procedure was presented as follows: In the typical synthesis, 3 mmol  $\text{Zn(NO}_3)_2 \cdot 6\text{H}_2\text{O}$ , and 7.2 mmol  $\text{C}_6\text{H}_5\text{Na}_3\text{O}_7 \cdot 2\text{H}_2\text{O}$  were dissolved in 60 mL distilled water under stirring from a uniform transparent solution. Then, 30 mmol NaOH was added to the mixture directly. After stirring for 120 min, the material was obtained by filtering and washing three to four times with distilled water and ethanol, and finally dried at 60 °C overnight.

### 2.3 Characterization

The powder X-ray diffraction (XRD) was carried out on a Bruker D8 Advance diffractometer (Germany) with the Cu  $K\alpha$  irradiation ( $\lambda = 1.54060$ ). The Fourier transform infrared spectroscopy (FTIR, Madison, WI, USA) measurement was performed to investigate the functional groups of  $\text{Zn(OH)}_2$ . Scan electron microscope (SEM, JEOL series 7600F) was used to explore the surface morphology and size of the sample.

### 2.4 Photodegradation of TCH by catalyst

The photocatalytic activity of  $\text{Zn(OH)}_2$  was examined by the decomposition of tetracycline hydrochloride (TCH). The experimental procedure was as follows: 50 mg catalyst was dispersed in a beaker of 250 mL containing 100 mL TCH 15 mg/L and stirred at 250 rpm continuously for 30 min in dark to get an adsorption/desorption equilibrium. Then the mixture was irradiated with a 250 W Xe lamp. At given time intervals, a certain suspension was filtered through a Millipore filter (0.45  $\mu\text{m}$  PTFE membrane) and measured residual TCH concentration by a UV-Vis spectrophotometer (Agilent 8453) at a maximum wavelength of 375 nm. The DE and rate constant of TCH were calculated according to the equation (1) and (2) respectively:

$$\text{DE} = \frac{C_0 - C_t}{C_0} \times 100\% \quad (1)$$

$$\ln \frac{C_0}{C_t} = kt \quad (2)$$

Where  $C_0$  and  $C_t$  are the concentration of TCH at initial ( $t = 0$ ) and time  $t$  (min), respectively.  $k$  is the pseudo first-order rate constant. The  $k$  value was calculated from the slope of the  $\ln (C_0/C_t) - t$  plots.

### 3 Results and discussion

#### 3.1 Characterization of material

The XRD pattern of the as-prepared sample is shown in Figure 1(a). The  $\epsilon$ -Zn(OH)<sub>2</sub> material was single phase with orthorhombic structure in accordance with reported data JCPDS card No. 38-0385<sup>(10)</sup>. Furthermore, diffraction peaks were sharp, and no impurity peaks demonstrated high crystallinity.

According to the IR spectra shown in Figure 1(b), the broad band centered at around 3250 cm<sup>-1</sup> is the O-H stretching modes from the two crystallographically independent OH groups in Zn(OH)<sub>2</sub>. The absorption peaks from 750 cm<sup>-1</sup> to 1200 cm<sup>-1</sup> could be attributed to the Zn-OH bends. The strong peak at 470 cm<sup>-1</sup> was related to the Zn-O stretch fall<sup>(11)</sup>.

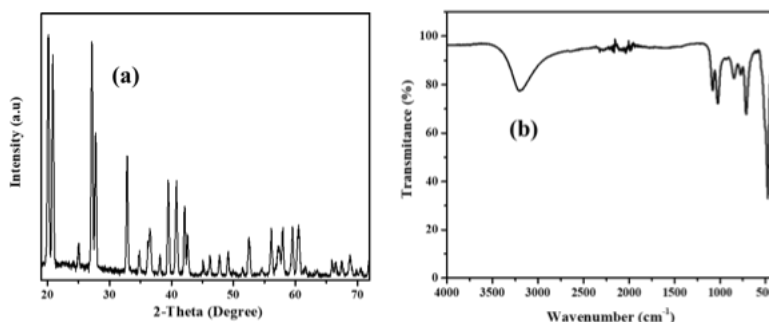


Fig 1. (a) XRD pattern and (b) IR spectra of Zn(OH)<sub>2</sub>

The SEM analysis of sample is presented in Figure 2. Zn(OH)<sub>2</sub> was observed to have a triangular prism morphology with a length prism of 5-7  $\mu$ m and triangle angles of 56.92, 69.46, and 66.71°. This result is consistent with the XRD spectral analysis.

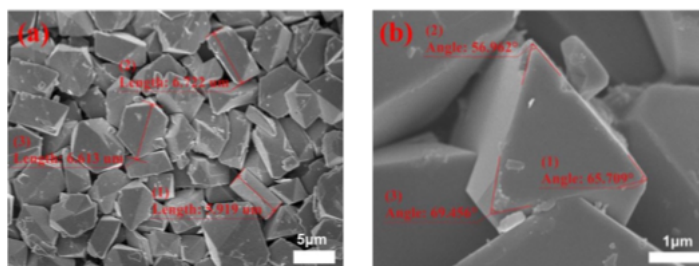


Fig 2. SEM images of Zn(OH)<sub>2</sub> with different scale bars

The results of HR-TEM and SEAD analysis are shown in Figure 3. It was seen that the Zn(OH)<sub>2</sub> particles with the size of about 5-10 nm (Figure 3(a)), were gathered together to form a triangular prism, as shown in the SEM results above. The crystal planes could be observed in Figure 3(b), the distance between the planes was 0.21 nm. Besides, planes (102), (110), (100), (002), and (101) are identified in Figure 3(c).

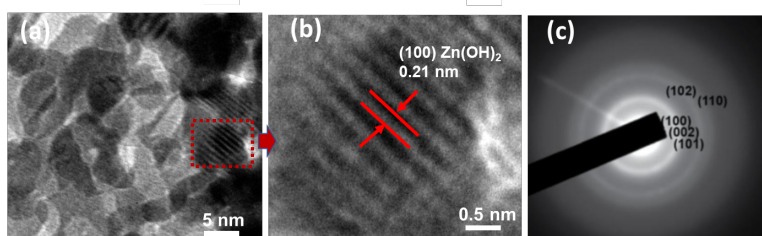


Fig 3. (a-b) HR-TEM and (b) SEAD images of  $\epsilon$ -Zn(OH)<sub>2</sub>

To investigate the light absorption and optical properties of the catalyst, the DRS/UV-Vis of the  $\text{Zn(OH)}_2$  sample was carried out, as shown in Figure 4(a). It exhibited a strongly absorb radiation in the region of 250-375 nm, these demonstrated photocatalytic ability in the UV region. Furthermore, the bandgap energy ( $E_g$ ) of the catalyst was also evaluated by Tauc's method<sup>(12)</sup>:

$$(\alpha h\nu)^2 = A \cdot (h\nu - E_g) \quad (3)$$

Where  $\alpha$  is the absorption coefficient,  $h\nu$  is the photon energy,  $A$  is a constant. The energy intersection of the curve of  $(\alpha h\nu)^2$  with respect to  $h\nu$  gives  $E_g$  when the linear region is extrapolated to the zero ordinate. Hence,  $E_g$  of  $\text{Zn(OH)}_2$  can be calculated to be 3.19 eV, as shown in Figure 4b.

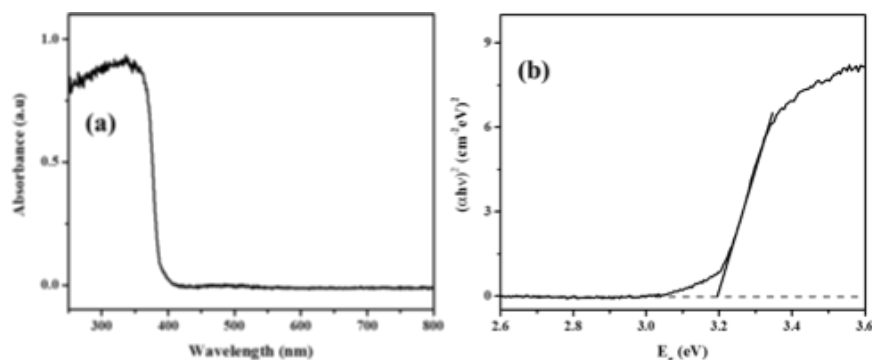


Fig 4. (a) UV-Vis diffuse reflectance spectra and (b) Tauc's plot of the  $\text{Zn(OH)}_2$

### 3.2 Photocatalytic activity

The initial TCH concentration was selected from 5 to 20 mg/L to examine their effect on the photocatalytic reaction, the results are shown in Figure 5. It could be found that the DE and reaction rate were decreased when increasing TCH concentration. The DE and reaction rate at the TCH concentration of 5 mg/L was the highest, exhibiting 89.51% and  $0.120 \text{ min}^{-1}$ , respectively. At a TCH concentration of 10 mg/L, the DE was 79.09 which was higher than that of 15 mg/L. However, both reaction rates were similar, showing  $0.084 \text{ min}^{-1}$ . The decrease in degradation might be due to the fact that more and more TCH molecules were adsorbed on the constant surface of catalytic, reducing the formation of hydroxyl radicals that assist the photocatalysis. Furthermore, at high initial TCH concentrations, penetration of photons into the solution is hindered, resulting in slower reaction rates<sup>(13)</sup>.

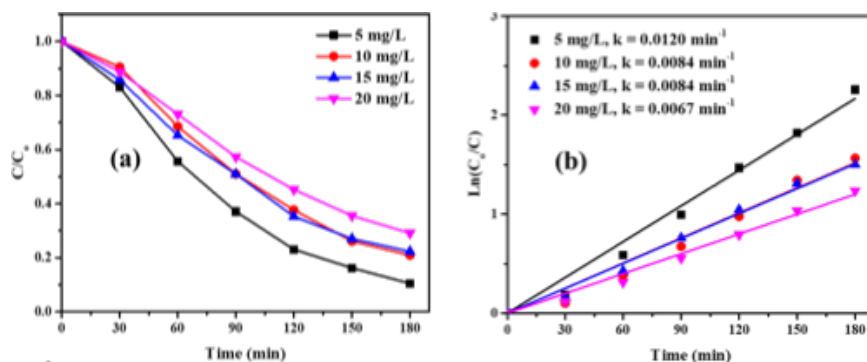


Fig 5. (a) Photocatalytic degradation performance in different initial TCH concentrations, (b) first-order kinetic plots

As seen in Figure 6(a), the TCH structure contains connected ring systems with multiple ionizable functional groups<sup>(14)</sup>. It has three pK<sub>a</sub>s and thus can exist the different TCH species. At a pH of below 3.3, TCH transforms into cationic species ( $\text{TCH}_3^+$ ) by the protonation of the dimethyl- ammonium group. When pH was between 3.3 and 7.3, TCH existed as zwitterionic species

(TCH<sup>0</sup>) due to the loss of a proton from the phenolic diketone moiety. At pH higher than 7.3, TCH changed into anionic species (TCH<sup>-</sup>, TCH<sup>2-</sup>), because of the loss of protons from the tri-carbonyl system and phenolic diketone moiety<sup>(15)</sup>. In addition, the UV-Vis spectra of TCH have shown a correlation between the increase in pH and the band shift of the antibiotic (Figure 6(b)).

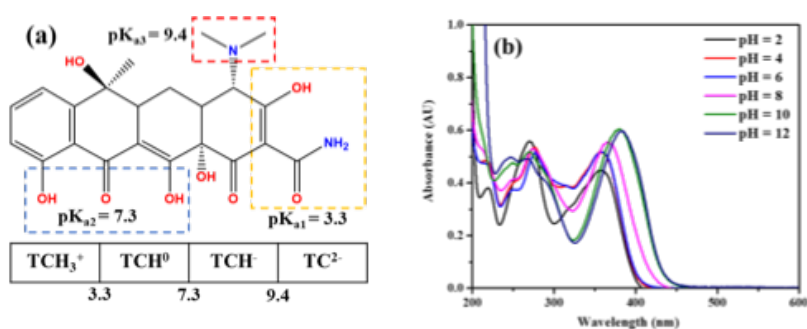


Fig 6. (a) Structure and pH-dependent surface speciation of TCH, (b) UV-vis absorption spectra of TCH at different pH

The degradation process of TCH was significantly dependent on the pH of the solution which affected the adsorbent surface charge, the form of ionization molecules. Solutions were prepared at a wide range of pH 2-12 to evaluate the influence of pH, the results are illustrated in Figure 7. At a pH of 2, the DE of TCH was negligible due to the protonation of Zn(OH)<sub>2</sub> in acidic media ( $\text{Zn(OH)}_2(\text{s}) + 2\text{H}^+(\text{aq}) \rightarrow \text{Zn}^{2+} + 2\text{H}_2\text{O}$ ). As the pH of the solution increases, the DE and rate constant both increased. At pH of 10 and 12, the DE was significantly decreased in 60 min, showing 80.25 and 82.33 % for 10 and 12, respectively. However, after that it slowly decreased, reaching 87.57 and 94.89% in 180 min for pH 10 and 12. This can be explained by following the reason: At higher pH, more and more •OH radicals were generated from OH<sup>-</sup> ions on the surface of the catalyst, leading to the enhanced decomposition of TCH. However, in an alkaline medium, the Zn(OH)<sub>2</sub> can be dissolved ( $\text{Zn(OH)}_2(\text{s}) + 2\text{OH}^-(\text{aq}) \rightarrow \text{ZnO}_2^{2-}(\text{aq}) + 2\text{H}_2\text{O}$ )<sup>(16)</sup>.

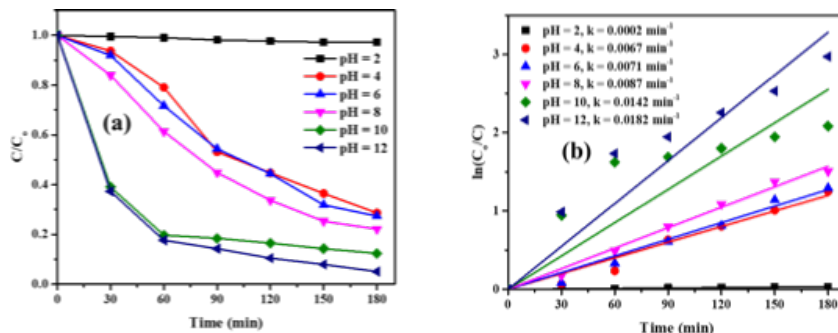


Fig 7. 7. (a) Photocatalytic degradation performance of Zn(OH)<sub>2</sub> in different pH conditions, (b) first-order kinetic plots

The plausible photocatalytic mechanism of Zn(OH)<sub>2</sub> for the decomposition process of TCH was illustrated in Figure 8. As photons strike the Zn(OH)<sub>2</sub> by visible light irradiation, the electrons in the valence band (VB) of Zn(OH)<sub>2</sub> were excited to move the conduction band (CB) with the formation of the same number of holes in the VB. Then the electrons in CB can reduce the absorbed oxygen molecules (O<sub>2</sub>) to generate superoxide radicals (•O<sub>2</sub><sup>-</sup>). Meanwhile, the photogenerated holes can react with H<sub>2</sub>O or hydroxyl (OH<sup>-</sup>) to generate hydroxyl radical (•OH). The produced •O<sub>2</sub><sup>-</sup> and •OH radicals play important role in the photocatalytic process<sup>(17)</sup>. These powerful radicals can rapidly degrade the TCH into intermediates and entirely decompose the TCH to CO<sub>2</sub>, and H<sub>2</sub>O<sup>(16)</sup>.

The catalyst after an experiment was recovered by filtering and washing with distilled water, then dried at 120 °C for 12 h to be used for the next experiment. The DE was decreased from 89.51 to 82.3 % after 1<sup>st</sup> reuse, however it remained relatively stable for subsequent uses. The DE was 79.1 % for 5<sup>th</sup> cyclic experiment, in Figure 9(a). The morphology of the catalyst after 5<sup>th</sup> cyclic experiment, in Figure 9(b), was similar to that of the original catalyst, in Figure 2(a). These showed that ε-Zn(OH)<sub>2</sub> has high stability and can be a potential catalyst for large-scale industrial applications.

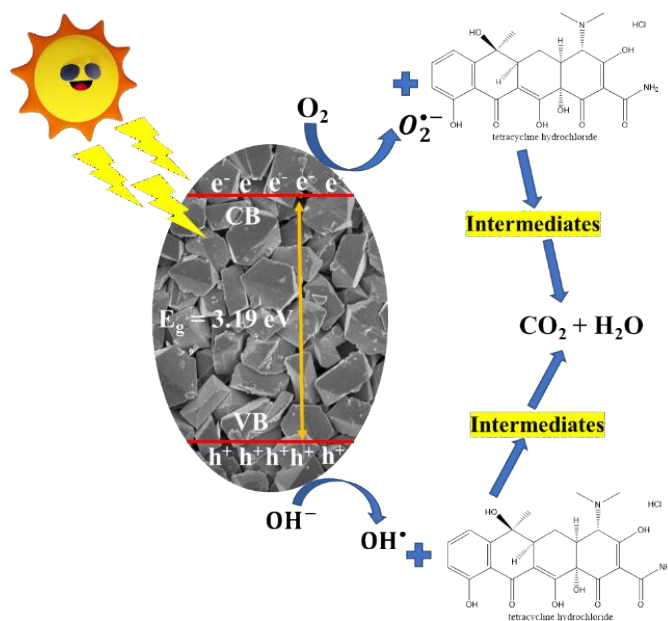


Fig 8. 8. Schematic diagram for the photocatalytic mechanism of  $\text{Zn(OH)}_2$

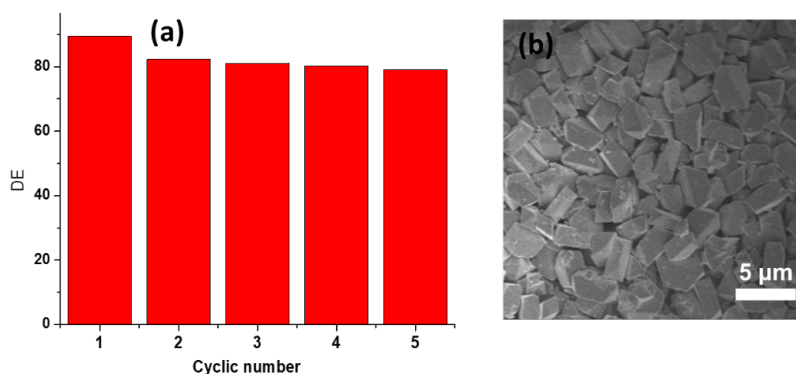


Fig 9. (a) Cyclic experiments and (b) SEM analysis of catalyst after 5<sup>th</sup> cyclic experiment

We already know that each type of catalyst has the corresponding optimal conditions for the decomposition of a certain organic substance. Therefore, it is difficult to compare the absolute efficiency of their performance. However, the indirect comparison of the performance of  $\epsilon\text{-Zn(OH)}_2$  with other catalysts is presented in Table 1. The degradation efficiency of THC in  $\epsilon\text{-Zn(OH)}_2$  was relatively high compared with other catalysts even though under visible light and without strong oxidizing agent  $\text{H}_2\text{O}_2$ . However, the degradation time of THC in  $\epsilon\text{-Zn(OH)}_2$  was longer than that of three-dimensional flower-like  $\text{TiO}_2/\text{TiOF}_2$ , and nanoparticles  $\text{ZnO}$  and shorter than nanoparticles  $\text{CdS-TiO}_2$ , nanocomposite  $\text{FeNi}_3/\text{SiO}_2/\text{CuS}$ .



**Table 1.** Comparison with other catalysts

Catalyst	Morphology	Reaction conditions	Performance	Ref.
ZnO/Zn(OH) <sub>2</sub>	Nanoparticles	Sunset yellow of 20 µg/mL, pH of 6.0, dosage of 1 g/L	Degradation of sunset yellow, DE of 92%, rate constant of 0.029 min <sup>-1</sup>	(18)
Zn(OH) <sub>2</sub>	Flake	RhB concentration of 5.0 mg/L, catalyst dosage of 150 mg/L, under UVC radiation	Degradation of RhB, DE of about 40%, rate constant of 0.05 min <sup>-1</sup>	(19)
TiO <sub>2</sub> /TiOF <sub>2</sub>	Three-dimensional flower-like	TCH concentration of 10 mg/L, catalyst dosage of 0.3 g/L, under xenon lamp	Degradation of TCH, DE of 85% in 30 min, rate constant of 0.025 min <sup>-1</sup>	(20)
ZnO	Nanoparticles	TC concentration of 50 mg/L, catalyst dosage of 1 g/L, under UV irradiation	Degradation of TC, DE of 96.1% in 120 min	(21)
FeNi <sub>3</sub> /SiO <sub>2</sub> /CuS	Nanocomposite	TC concentration of 20 mg/L, catalyst dosage of 0.005 g/L, pH of 9, Xenon light	Degradation of TC, DE of 81% in 200 min	(22)
In <sub>2</sub> S <sub>3</sub> /Bi <sub>2</sub> WO <sub>6</sub>	Core-shell	TCH concentration of 20 mg/L, catalyst dosage of 0.5 g/L, under visible light irradiation	Degradation TCH, DE of 96%, 0.017 min <sup>-1</sup>	(23)
CdS-TiO <sub>2</sub>	Nanoparticles	TCH concentration of 50 mg/L, catalyst dosage of 1 g/L, Under xenon lamp	Degradation of TCH, DE of 87.06% in 8h	(24)
(Bi)BiOBr/rGO	Hierarchical microspherical structures	TC concentration of 20 mg/L dosage catalyst of 1 g/L, Xenon lamp	Degradation of tetracycline, DE of 75.5%,	(25)
ε-Zn(OH) <sub>2</sub>	Triangular prism	TCH concentration of 20 mg/L, catalyst content of 0.5 g/L, pH solution of 12, under visible light	Degradation of TCH, DE of 97.52 % in 180 min, rate constant of 0.120 min <sup>-1</sup>	This study

## 4 Conclusion

The ε-Zn(OH)<sub>2</sub> material has been successfully prepared by the simple precipitation method. The morphology of ε-Zn(OH)<sub>2</sub> has been demonstrated that to be the special morphology compared with that of Zn(OH)<sub>2</sub> in other studies. ε-Zn(OH)<sub>2</sub> was a triangular prism with a length prism of 5-7 µm and triangle angles of 56.92, 69.46, and 66.71°. It had a narrow bandgap (3.19 eV) and exhibited a strongly absorption of radiation in the UV region. The decomposition rate of THC in ε-Zn(OH)<sub>2</sub> was fast, showing the DE of 97.52%, rate constant of 0.120 min<sup>-1</sup> in 180 min at pH of 12 under visible irradiation. This study proved that morphology has a strong affect to the physical properties and catalytic efficiency of Zn(OH)<sub>2</sub>. As the result, its catalytic efficiency was higher than that of nanoparticles, flowers, and flakes photocatalysts. It proved to be a potential catalyst for the treatment of antibiotics in aqueous medium.

## Acknowledgments

The authors are grateful for the financial support from Vietnam National Foundation for Science and Technology Development (NAFOSTED) under grant number 104.05-2018.333.

## References

- Hoslett J, Ghazal H, Katsou E, Jouhara H. The removal of tetracycline from water using biochar produced from agricultural discarded material. *Science of The Total Environment*. 2021;2021(751):141755. Available from: <https://doi.org/https://doi.org/10.1016/j.scitotenv.2020.141755>.
- Samadi-Maybodi A, Khabazifard R. Photodegradation of tetracycline and doxycycline under visible radiation using MIL-MIL101Fe (NH<sub>2</sub>) @g-C<sub>3</sub>N<sub>4</sub>@CoFe<sub>2</sub>O<sub>4</sub>/GO as photocatalyst. *Optik*. 2022;262:168934. Available from: <https://doi.org/https://doi.org/10.1016/j.ijleo.2022.168934>.
- Yang J, Han L, Yang W, Liu Q, Fei Z, Chen X, et al. In situ synthetic hierarchical porous MIL-53(Cr) as an efficient adsorbent for mesopores-controlled adsorption of tetracycline. *Microporous and Mesoporous Materials*. 2022;332(111667). Available from: <https://doi.org/https://doi.org/10.1016/j.micromeso.2021.111667>.
- Zyła R, Ledakowicz S, Boruta T, Olak-Kucharczyk M, Foszpańczyk M, Mrozińska Z, et al. Removal of Tetracycline Oxidation Products in the Nanofiltration Process. *Water*. 2021;13(4):555. Available from: <https://doi.org/10.3390/w13040555>.
- Zhang S, Zheng K, Xu G, Liang B, Yin Q. Enhanced removal of tetracycline via advanced oxidation of sodium persulfate and biochar adsorption. *Environmental Science and Pollution Research*. 2022;29(48):72556–72567. Available from: <https://doi.org/10.1007/s11356-022-20817-7>.
- Li Y, Zhang Q, Lu Y, Song Z, Wang C, Li D, et al. Surface hydroxylation of TiO<sub>2</sub>/g-C<sub>3</sub>N<sub>4</sub> photocatalyst for photo-Fenton degradation of tetracycline. *Ceramics International*. 2022;48(1):1306–1313. Available from: <https://doi.org/https://doi.org/10.1016/j.ceramint.2021.09.215>.
- He X, Kai T, Ding P. Heterojunction photocatalysts for degradation of the tetracycline antibiotic: a review. *Environmental Chemistry Letters*. 2021;19(6):4563–4601. Available from: <https://doi.org/10.1007/s10311-021-01295-8>.

- 8) Rocha RLP, Honorio LMC, Bezerra RDDS, Trigueiro P, Duarte TM, Fonseca MG, et al. Light-Activated Hydroxyapatite Photocatalysts: New Environmentally-Friendly Materials to Mitigate Pollutants. *Minerals*. 2022;12(5):525. Available from: <https://doi.org/10.3390/min12050525>.
- 9) Yang Y, Meng S, Zheng X, Wu H, Fu X, Chen S. The morphology and photocatalytic performance of Zn(OH)F under different synthetic conditions. *Journal of Fluorine Chemistry*. 2020;237(109600). Available from: <https://doi.org/https://doi.org/10.1016/j.jfluchem.2020.109600>.
- 10) Donia DT, Bauer EM, Missori M, Roselli L, Cecchetti D, Tagliatesta P, et al. Room Temperature Syntheses of ZnO and Their Structures. 2021;13(733). Available from: <https://doi.org/10.3390/sym13040733>.
- 11) Gordeeva A, Hsu YJ, Jenei IZ, Carvalho PHBB, Simak SI, Andersson O, et al. Layered Zinc Hydroxide Dihydrate,  $\text{Zn}_{0.5}(\text{OH})_{10} \cdot 2\text{H}_2\text{O}$ , from Hydrothermal Conversion of  $\epsilon\text{-Zn}(\text{OH})_2$  at Gigapascal Pressures and its Transformation to Nanocrystalline ZnO. *ACS Omega*. 2020;5(28):17617–17627. Available from: <https://doi.org/10.1021/acsomega.0c02075>.
- 12) Pham TAT, Van Anh Tran, Van Duong Le, Nguyen MV, Truong DD, Do XT, et al. Facile Preparation of ZnO Nanoparticles and Ag/ZnO Nanocomposite and Their Photocatalytic Activities under Visible Light. *International Journal of Photoenergy*. 2020;2020:1–14. Available from: <https://doi.org/10.1155/2020/8897667>.
- 13) Kaushik B, Yadav S, Rana P, Rana P, Solanki K, Rawat D. Precisely engineered type II ZnO-CuS based heterostructure: A visible light driven photocatalyst for efficient mineralization of organic dyes. *Applied Surface Science*. 2022;590(153053). Available from: <https://doi.org/https://doi.org/10.1016/j.apsusc.2022.153053>.
- 14) Wang L, Hu A, Liu H, Yu K, Wang S, Deng X, et al. Degradation of tetracycline hydrochloride (TCH) by active photocatalyst rich in oxygen vacancies: Performance, transformation product and mechanism. *Applied Surface Science*. 2022;589(152902). Available from: <https://doi.org/https://doi.org/10.1016/j.apsusc.2022.152902>.
- 15) Cheng J, Xie Y, Wei Y, Xie D, Sun W, Zhang Y, et al. Degradation of tetracycline hydrochloride in aqueous via combined dielectric barrier discharge plasma and Fe–Mn doped AC. *Chemosphere*. 2022;286(131841). Available from: <https://doi.org/10.1016/j.chemosphere.2021.131841>.
- 16) Vu AT, Pham TAT, Do XT, Van Anh Tran, Van Duong Le, Truong DD, et al. Preparation of Hierarchical Structure Au/ZnO Composite for Enhanced Photocatalytic Performance: Characterization, Effects of Reaction Parameters, and Oxidizing Agent Investigations. *Adsorption Science & Technology*. 2021;2021:1–19. Available from: <https://doi.org/10.1155/2021/5201497>.
- 17) Uribe-López MC, Hidalgo-López MC, López-González R, Frías-Márquez DM, Núñez-Nogueira G, Hernández-Castillo D, et al. Photocatalytic activity of ZnO nanoparticles and the role of the synthesis method on their physical and chemical properties. *Journal of Photochemistry and Photobiology A: Chemistry*. 2021;404(112866). Available from: <https://doi.org/https://doi.org/10.1016/j.jphotochem.2020.112866>.
- 18) Faheem M, Siddiqi HM, Habib A, Shahid M, Afzal A. ZnO/Zn(OH)<sub>2</sub> nanoparticles and self-cleaning coatings for the photocatalytic degradation of organic pollutants. *Frontiers in Environmental Science*. 2022;10:1–09. Available from: <https://doi.org/https://doi.org/10.3389/fenvs.2022.965925>.
- 19) Lopes OF, De Mendonça VR, Umar A, Chuahan MS, Kumar R, Chauhan S, et al. Zinc hydroxide/oxide and zinc hydroxy stannate photocatalysts as potential scaffolds for environmental remediation. *New Journal of Chemistry*. 2015;39(6):4624–4630. Available from: <https://doi.org/10.1039/C5NJ00324E>.
- 20) Hou C, Liu H, Li Y. The preparation of three-dimensional flower-like  $\text{TiO}_{0.2}/\text{TiOF}_{0.2}$  photocatalyst and its efficient degradation of tetracycline hydrochloride. *RSC Advances*. 2021;11(25):14957–14969. Available from: <https://doi.org/10.1039/D1RA01772A>.
- 21) Ari H, Adewole AO, Ugya AY, Asipita OH, Musa MA, Feng W. Biogenic fabrication and enhanced photocatalytic degradation of tetracycline by bio structured ZnO nanoparticles. *Environmental Technology*. 2021;p. 1–16. Available from: <https://doi.org/10.1080/09593330.2021.2001049>.
- 22) Nasseh N, Barikbin B, Taghavi L. Photocatalytic degradation of tetracycline hydrochloride by FeNi<sub>3</sub>/SiO<sub>2</sub>/CuS magnetic nanocomposite under simulated solar irradiation: Efficiency, stability, kinetic and pathway study. *Environmental Technology & Innovation*. 2020;20(101035). Available from: <https://doi.org/https://doi.org/10.1016/j.eti.2020.101035>.
- 23) He Z, Siddique MS, Yang H, Xia Y, Su J, Tang B, et al. Novel Z-scheme In<sub>2</sub>S<sub>3</sub>/Bi<sub>2</sub>WO<sub>6</sub> core-shell heterojunctions with synergistic enhanced photocatalytic degradation of tetracycline hydrochloride. *Journal of Cleaner Production*. 2022;339(130634). Available from: <https://doi.org/https://doi.org/10.1016/j.jclepro.2022.130634>.
- 24) Li W, Ding H, Ji H, Dai W, Guo J, Du G. Photocatalytic Degradation of Tetracycline Hydrochloride via a CdS-TiO<sub>2</sub> Heterostructure Composite under Visible Light Irradiation. *Nanomaterials*. 2018;8(6):415. Available from: <https://doi.org/10.3390/nano8060415>.
- 25) Jiang H, Wang Q, Chen P, Zheng H, Shi J, Shu H, et al. Photocatalytic degradation of tetracycline by using a regenerable (Bi)BiOBr/rGO composite. *Journal of Cleaner Production*. 2022;339(130771). Available from: <https://doi.org/https://doi.org/10.1016/j.jclepro.2022.130771>.